arXiv:cond-mat/0509412v1 [cond-mat.str-el] 15 Sep 2005

Magnetic and superconducting correlations in the two-dimensional Hubbard model

W. Metzner, J. Reiss, D. Rohe
Max Planck Institute for Solid State Research
Heisenbergstr. 1, D-70569 Stuttgart, Germany

February 2, 2008

Key words Hubbard Model, Renormalization Group
PACS 71.10.Hf

Abstract

The interplay and competition of magnetic and superconducting correlations in the weakly interacting two-dimensional Hubbard Model is investigated by means of the functional renormalization group. At zero temperature the flow of interactions in one-loop approximation evolves into a strong coupling regime at low energy scales, signalling the possible onset of spontaneous symmetry breaking. This is further analyzed by a mean-field treatment of the strong renormalized interactions which takes into account magnetic and superconducting order simultaneously. The effect of strong correlations on single-particle properties in the normal phase is studied by calculating the flow of the self-energy.

1 Introduction

The two-dimensional Hubbard model has been proposed by Anderson [1] as a basic model for the electronic degrees of freedom in the copper-oxide planes of high-temperature superconductors. In agreement with the generic phase diagram of the cuprates, the Hubbard model exhibits antiferromagnetic order at half-filling, and is expected to become a d-wave superconductor near half-filling in two dimensions [2]. The exchange of antiferromagnetic spin fluctuations has been suggested as a plausible mechanism leading to d-wave pairing [3, 4, 5]. In this picture the BCS effective interaction $V_{\mathbf{k}\mathbf{k}'}$ is roughly proportional to the spin correlation function $\chi_s(\mathbf{k}-\mathbf{k}')$. Close to half-filling, $\chi_s(\mathbf{q})$ has a pronounced maximum at the antiferromagnetic wave vector (π,π). As a consequence, the gap equation with $V_{\mathbf{k}\mathbf{k}'}$ as input has a solution with $d_{x^2-y^2}$-wave symmetry, such that the gap $\Delta_{\mathbf{k}}$ has maximal modulus but opposite sign near the points $(\pi,0)$ and $(0,\pi)$ in the

Brillouin zone, respectively. This intuitive argument has been corroborated by a self-consistent perturbative solution of the two-dimensional Hubbard model within the so-called fluctuation-exchange approximation [6].

The spin-fluctuation mechanism for pairing could in principle be spoiled by other contributions to the BCS interactions and also by spin density wave instabilities. Unfortunately, it is hard to prove the existence of superconductivity in the Hubbard model by exact numerical computation [2, 7], as a consequence of finite size and/or temperature limitations. However, the tendency towards antiferromagnetism and d-wave pairing is captured already by the 2D Hubbard model at *weak* coupling, where one can hope to proceed by perturbative calculations. Conventional perturbation theory breaks down for densities close to half-filling, since competing infrared divergences appear as a consequence of Fermi surface nesting and van Hove singularities [8, 9, 10]. A controlled and unbiased treatment of these divergencies cannot be achieved by standard resummations of Feynman diagrams, but requires a renormalization group (RG) analysis which takes into account the particle-particle and particle-hole channels on an equal footing. In the following we describe progress in this direction achieved by applying the socalled *functional renormalization group* (fRG) to the two-dimensional Hubbard model.

In Sec. 2 we define the two-dimensional Hubbard model and describe the relevant infrared singularities in perturbation theory. In Sec. 3 we briefly review the Wick ordered version of the functional renormalization group and discuss the one-loop flow of effective interactions and susceptibilities for the Hubbard model. In Sec. 4 we compute the flow of the electronic self-energy and discuss how the strong correlations at low energy scales affect spectral properties of single-particle excitations. In Sec. 5 we treat the effective low-energy problem obtained from the fRG flow at zero temperature within a mean-field approximation and find a range of fillings where magnetic and and sizable superconducting order coexist. A short conclusion follows in Sec. 6.

2 Two-dimensional Hubbard Model

The Hubbard model describes tight-binding electrons with a local repulsion $U > 0$. The Hamiltonian reads

$$H = \sum_{\mathbf{i},\mathbf{j}} \sum_{\sigma} t_{\mathbf{ij}}\, c^{\dagger}_{\mathbf{i}\sigma} c_{\mathbf{j}\sigma} + U \sum_{\mathbf{j}} n_{\mathbf{j}\uparrow} n_{\mathbf{j}\downarrow} \,, \tag{1}$$

where $c^{\dagger}_{\mathbf{i}\sigma}$ and $c_{\mathbf{i}\sigma}$ are creation and annihilation operators for fermions with spin projection $\sigma = \uparrow, \downarrow$ on a lattice site $\mathbf{i}$, and $n_{\mathbf{j}\sigma} = c^{\dagger}_{\mathbf{j}\sigma} c_{\mathbf{j}\sigma}$. A hopping amplitude $-t$ between nearest neighbors and an amplitude $-t'$ between next-nearest neighbors on a square lattice leads to the dispersion relation

$$\epsilon_{\mathbf{k}} = -2t(\cos k_x + \cos k_y) - 4t'(\cos k_x \, \cos k_y) \tag{2}$$

for single-particle states. This dispersion relation has saddle points at $\mathbf{k} = (0, \pi)$ and $(\pi, 0)$, which lead to logarithmic van Hove singularities in the non-interacting density of states at the energy $\epsilon_{\rm vH} = 4t'$.

For a chemical potential $\mu = \epsilon_{\rm vH}$ the Fermi surface contains the van Hove points. In this case a perturbative calculation of the two-particle vertex function leads to several infrared divergencies already at second order in U, that is at one-loop level [8, 9, 10]. In particular, the particle-particle channel diverges as $\log^2$ for vanishing total momentum $\mathbf{k}_1 + \mathbf{k}_2$, and logarithmically for $\mathbf{k}_1 + \mathbf{k}_2 = (\pi, \pi)$. The particle-hole channel diverges logarithmically for vanishing momentum transfer; for momentum transfer (π, π) it diverges logarithmically if $t' \neq 0$ and as $\log^2$ in the special case $t' = 0$. Note that $\mu = 0$ for $t' = 0$ corresponds to half-filling ($n = 1$). In this case there are also logarithmic divergences for all momentum transfers parallel to (π, π) or $(\pi, -\pi)$ due to the strong nesting of the square shaped Fermi surface. For $\mu \neq \epsilon_{\rm vH}$ only the usual logarithmic Cooper singularity at zero total momentum in the particle-particle channel remains. However, the additional singularities at $\mu = \epsilon_{\rm vH}$ lead clearly to largely enhanced contributions for small $|\mu - \epsilon_{\rm vH}|$, especially if t' is also small.

Hence, for small $|\mu - \epsilon_{\rm vH}|$ one has to deal with competing divergencies in different channels. This problem calls for a renormalization group treatment.

3 Renormalization Group Approach

Early RG studies of the two-dimensional Hubbard model started with simple scaling approaches, very shortly after the discovery of high-T_c superconductivity [8, 9, 10]. These studies focused on dominant scattering processes between van Hove points in k-space, for which a small number of running couplings could be defined and computed on one-loop level. Spin-density and superconducting instabilities were identified from divergencies of the corresponding correlation functions.

A complete treatment of all scattering processes in the Brillouin zone is rather complicated since the effective interactions cannot be parametrized accurately by a small number of variables, even if irrelevant momentum and energy dependences are neglected. The *tangential* momentum dependence of effective interactions along the Fermi surface is strong and important in the low-energy limit. Hence, one has to deal with the renormalization of coupling *functions*. This problem is treated most naturally within a Wilsonian momentum shell RG [11], where modes are integrated out successively from high energy states down to the Fermi surface [12]. This type of RG is also the basis for important rigorous work on two-dimensional Fermi systems [13]. The successive integration of modes can be formulated as an exact hierarchy of flow equations for effective interactions (one-particle, two-particle etc.), which is known as the *exact* or *functional* renormalization

group [14, 15, 16]. Starting with the work of Zanchi and Schulz [17], several groups have computed effective interactions and susceptibilities for the two-dimensional Hubbard model, using various versions of the fRG in one-loop approximation [18, 19]. Here we focus on results obtained from the Wick-ordered version of the fRG [13]. Other versions yield qualitatively similar results.

3.1 Wick ordered flow equations

The renormalization group equations are obtained as follows (for details, see Salmhofer [13] and Ref. [18]). The infrared singularities are regularized by introducing an infrared cutoff $\Lambda > 0$ into the bare propagator such that contributions from momenta with $|\epsilon_{\mathbf{k}} - \mu| < \Lambda$ are suppressed. All Green functions of the interacting system will then depend on Λ, and the true theory is recovered only in the limit $\Lambda \to 0$. The RG equations are most conveniently obtained from the effective potential $\mathcal{V}^\Lambda$, which is the generating functional for connected Green functions with bare propagators amputated from the external legs. Taking a Λ-derivative one obtains an exact functional flow equation for this quantity. Expanding $\mathcal{V}^\Lambda$ on both sides of the flow equation in powers of the fermionic fields (i.e. Grassmann variables), and comparing coefficients, one obtains the so-called Polchinski equations [15] for the effective m-body interactions used by Zanchi and Schulz [17]. Salmhofer [13] has pointed out that an alternative expansion in terms of *Wick ordered* monomials of fermion fields yields flow equations for the corresponding m-body interactions V_m^Λ with a particularly simple structure (see Fig. 1). The flow

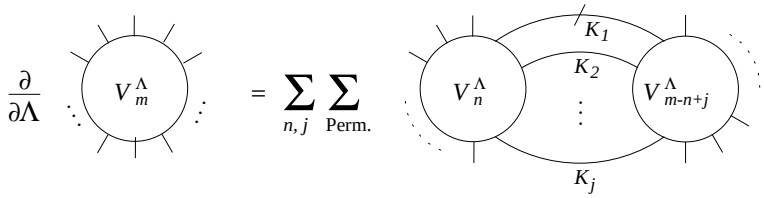

Figure 1: Diagrammatic representation of the flow equation for V_m^Λ in the Wick ordered version of the fRG. The line with a slash corresponds to $\partial D^\Lambda/\partial\Lambda$, the others to D^Λ; all possible pairings leaving m incoming and m outgoing external legs have to be summed.

of V_m^Λ is given as a bilinear form of other n-body interactions (at the same scale Λ), which are connected by lines corresponding to the propagator

$$D^\Lambda(k) = \frac{\Theta(\Lambda - |\xi_{\mathbf{k}}|)}{ik_0 - \xi_{\mathbf{k}}} \,, \tag{3}$$

where $\xi_{\mathbf{k}} = \epsilon_{\mathbf{k}} - \mu$, and one line corresponding to $\partial D^\Lambda(k)/\partial\Lambda$. For small Λ, the momentum integrals on the right hand side of the flow equation are thus

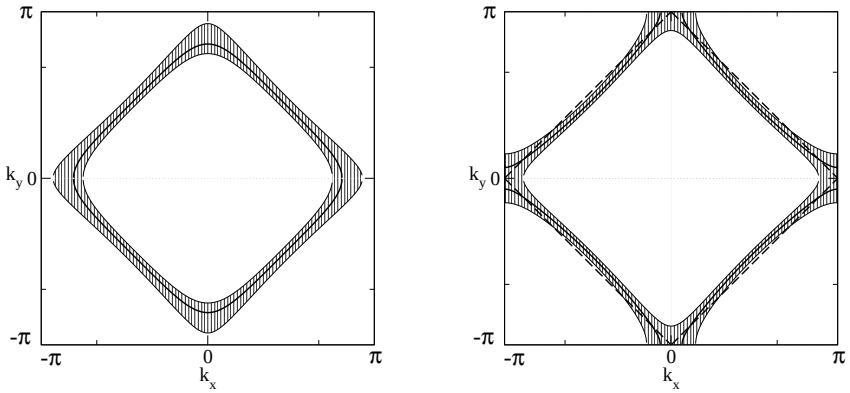

Figure 2: Fermi surfaces (solid lines) and support of the propagator D^Λ (shaded regions) in momentum space; *left*: $t' = 0$, *right*: $t' > 0$. The Fermi surface on the right intersects the socalled umklapp surface (dashed line).

restricted to momenta close to the Fermi surface (see Fig. 2). With the initial condition $\mathcal{V}^{\Lambda_0}$ = bare interaction, where $\Lambda_0 = \max|\xi_{\mathbf{k}}|$, the above flow equations determine the *exact* flow of the effective interactions as Λ sweeps over the entire energy range from the band edges down to the Fermi surface. The *effective* low-energy theory can thus be computed directly from the *microscopic* theory without introducing any ad hoc parameters. The structure of these flow equations is very convenient for a power counting analysis to arbitrary loop order [13], and also for a concrete numerical solution.

3.2 One-loop flow

To detect instabilities of the system in the weak-coupling limit, it is sufficient to truncate the infinite hierarchy of flow equations described by Fig. 1 at *one-loop* level, and neglect all components of the effective interaction except the two-particle interaction V_2^Λ. The effective two-particle interaction V_2^Λ then reduces to the one-particle irreducible two-particle vertex Γ^Λ, and its flow is determined by Γ^Λ itself (no other m-body interactions enter). Putting arrows on the lines to distinguish creation and annihilation operators one thus obtains the flow equation for Γ^Λ shown graphically in Fig. 3. Flow equations for *susceptibilities* are obtained by considering the exact fRG equations in the presence of suitable external fields, which leads to an additional one-body term in the bare interaction, and expanding everything in powers of the external fields to sufficiently high order [18]. On one-loop level one obtains the flow equations shown in Fig. 4. The flow of a susceptibility χ^Λ is determined by the corresponding response vertex R^Λ, the flow of which is in turn given by Γ^Λ and R^Λ itself. The initial conditions are given

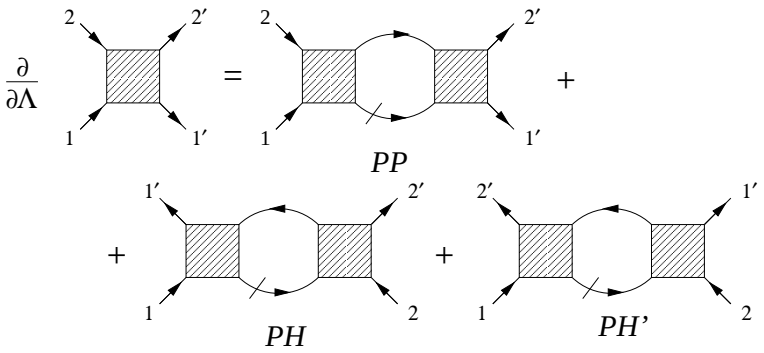

Figure 3: Flow equation for the two-particle vertex Γ^Λ in one-loop approximation with the particle-particle channel (PP) and the two particle-hole channels (PH and PH').

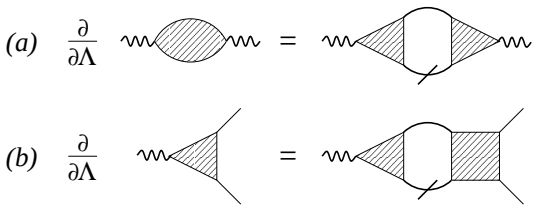

Figure 4: Flow equations for (a) the susceptibilities χ^Λ and (b) the response vertices R^Λ in one-loop approximation.

by $\chi^{\Lambda_0} = 0$ for the susceptibilities and by the bare response vertices for R^Λ. For pairing susceptibilities only the particle-particle channel contributes to the propagator pair in Fig. 4, for charge and spin density susceptibilities only the particle-hole channel.

It is clearly impossible to solve the flow equations with the full energy and momentum dependence of the two-particle vertex, since Γ^Λ has three independent energy and momentum variables. The problem can however be simplified by ignoring dependences which are *irrelevant* (in the RG sense) in the low energy limit, namely the energy dependence and the momentum dependence normal to the Fermi surface. Hence, we compute the flow of the two-particle vertex at zero energy and with at least three momenta on the Fermi surface (the fourth being determined by momentum conservation). On the right hand side of the flow equation we approximate the vertex by its zero energy value with three momenta projected on the Fermi surface (if not already there), as indicated in Fig. 5. This projection procedure is exact for the bare Hubbard vertex, and asymptotically exact in the low-energy regime, since only irrelevant dependences are neglected. The remaining tangential momentum dependence is discretized. The momentum-dependence of the two-particle vertex is thus approximated by a step function which is constant

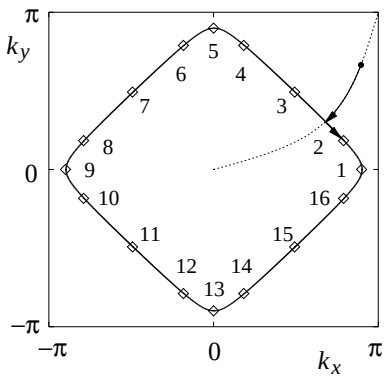

Figure 5: Projection of momenta on the Fermi surface; discretization and labelling of angle variables.

on "patches" (sectors) in the Brillouin zone.

The flow of the two-particle vertex has been computed for many different model parameters t' and U (t just fixes the absolute energy scale) and densities close to half-filling. At $T = 0$ the vertex develops a strong momentum dependence for small Λ with divergencies for several momenta at some critical scale $\Lambda_c > 0$, which vanishes exponentially for $U \to 0$. To see which physical instability is associated with the diverging two-particle vertex, various susceptibilities have been computed, in particular: commensurate and incommensurate spin susceptibilities $\chi_S(\mathbf{q})$ with $\mathbf{q} = (\pi, \pi)$, $\mathbf{q} = (\pi - \delta, \pi)$ and $\mathbf{q} = (1 - \delta)(\pi, \pi)$, where δ is a function of density [21], the commensurate charge susceptibility $\chi_C((\pi, \pi))$, and singlet pair susceptibilities with form factors

$$d(\mathbf{k}) = \begin{cases} 1 & (s\text{-wave}) \\ \frac{1}{\sqrt{2}}(\cos k_x + \cos k_y) & (\text{extended } s\text{-wave}) \\ \frac{1}{\sqrt{2}}(\cos k_x - \cos k_y) & (d\text{-wave } d_{x^2-y^2}) \\ \sin k_x \sin k_y & (d\text{-wave } d_{xy}). \end{cases} . \tag{4}$$

Some of these susceptibilities diverge together with the two-particle vertex at the scale Λ_c. Depending on the choice of U, t' and μ the strongest divergence is found for the commensurate or incommensurate spin susceptibility or for the pair susceptibility with $d_{x^2-y^2}$ symmetry. In Fig. 6 we show a typical result for the flow of the two-particle vertex and susceptibilities as a function of Λ. Only the singlet part (from a spin singlet-triplet decomposition) of the vertex is plotted, for various choices of the three independent external momenta. The triplet part flows generally more weakly than the singlet part. Note the threshold at $\Lambda = 2|\mu|$ below which the amplitudes for various scattering processes, especially umklapp scattering, renormalize only very slowly. The flow of the antiferromagnetic spin susceptibility is cut off at the same scale. The infinite slope singularity in some of the flow curves at

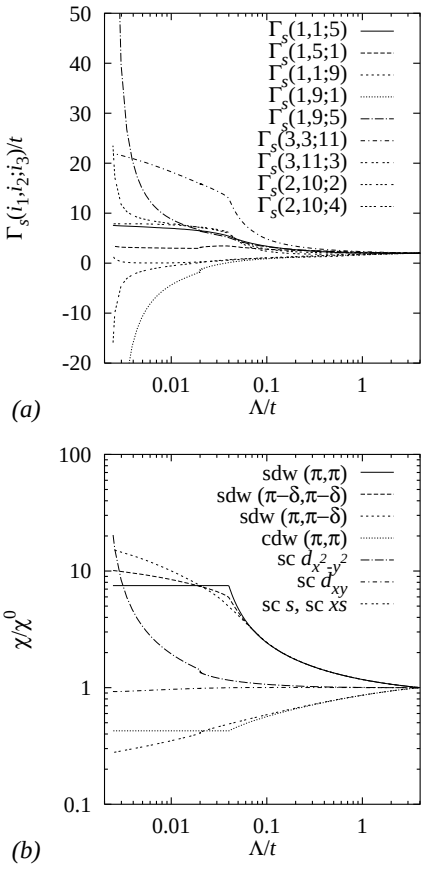

Figure 6: (a) The flow of the singlet vertex Γ_s^Λ as a function of Λ for several choices of the momenta $\mathbf{k}_{F1}$, $\mathbf{k}_{F2}$ and $\mathbf{k}'_{F1}$, which are labelled according to the numbers in Fig. 5. The model parameters are $U = t$ and $t' = 0$, the chemical potential is $\mu = -0.02t$; (b) the flow of the ratio of interacting and non-interacting susceptibilities, $\chi^\Lambda/\chi_0^\Lambda$, for the same system [from Ref. [18]].

scale $\Lambda = |\mu|$ is due to the van Hove singularity being crossed at that scale. The *pairing susceptibility* with $d_{x^2-y^2}$-symmetry is obviously *dominant* here (note the logarithmic scale). Following the flow of the two-particle vertex and susceptibilities, one can see that those interaction processes which enhance the antiferromagnetic spin susceptibility (especially umklapp scattering) also build up an attractive interaction in the $d_{x^2-y^2}$ pairing channel. This confirms the spin-fluctuation route to d-wave superconductivity [2]. Similar results leading to the same conclusions have been obtained by other one-loop calculations using different versions of the fRG [17, 19, 20].

4 Two-loop self-energy

The self-energy Σ for the 2D Hubbard model, which encodes the influence of correlations on single-particle excitations, has been analyzed within the functional RG framework in several recent articles. Interesting dynamical contributions to the self-energy set in at second order in the two-particle interactions, corresponding to the two-loop diagram shown in Fig. 7. The

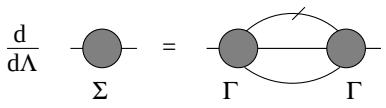

Figure 7: Flow equation for the two-loop self energy.

vertices on the right-hand side were obtained from the one-loop flow equation. A full two-loop calculation, including two-loop vertex renormalization, would be very complex, and has not been done so far.

Some of the earlier studies focused on the frequency derivative of the self-energy on the Fermi surface, which determines the wave function renormalization factor $Z = [1 - \partial_\omega \mathrm{Re}\Sigma(\mathbf{k}_F, \omega)|_{\omega=0}]^{-1}$. In Fermi liquids Z yields the weight of the quasi-particle peak in the spectral function. Zanchi [22] computed the flow of Z for the 2D Hubbard model with pure nearest neighbor hopping at half-filling and found that Z is strongly reduced when the renormalized interactions increase, the suppression being strongest near the van Hove points. Subsequently, Honerkamp and Salmhofer [23] computed the flow of the Z-factor at and also away from half-filling. While confirming an anisotropic reduction of Z, they observed that this suppression evolves much slower than the divergence of dominant interactions. In addition, they pointed out that the self-energy does not significantly affect the vertex renormalization in the perturbative regime, that is before the interactions become very strong. The imaginary part of the self-energy at zero frequency, $\mathrm{Im}\Sigma(\mathbf{k}_F, 0)$, was computed by Honerkamp [24]. In Fermi liquids this quantity is directly related to the decay rate of quasi-particles. For a hole-doped Hubbard model with a concave Fermi surface that almost touches the van Hove points (this requires a negative t') he found that $\mathrm{Im}\Sigma(\mathbf{k}_F, 0)$ is moderately anisotropic, with larger values for momenta closer to the van Hove points.

Functional RG calculations of the full frequency dependence of the self-energy were performed recently by Katanin and Kampf [25] within the one-particle irreducible version of the fRG, and by two of us [26] within the Wick ordered version. The real and imaginary parts of $\Sigma(\mathbf{k}_F, \omega)$ and the resulting spectral function $A(\mathbf{k}_F, \omega)$ were computed for the 2D Hubbard model with nearest and next-to-nearest neighbor hopping at finite temperature, which was chosen such that the largest renormalized interactions were strongly enhanced, but did not diverge for $\Lambda \to 0$. Marked deviations from Fermi

liquid behavior were obtained for $\mathbf{k}_F$ close to a van Hove point, and also near other hot spots [27] in the case of filling factors above the van Hove singularity: the imaginary part of $\Sigma(\mathbf{k}_F, \omega)$ develops a pronounced peak at low frequencies, as seen for example in Fig. 8, which leads to a double-peak structure in the spectral functions, reminiscent of a pseudogap. This double

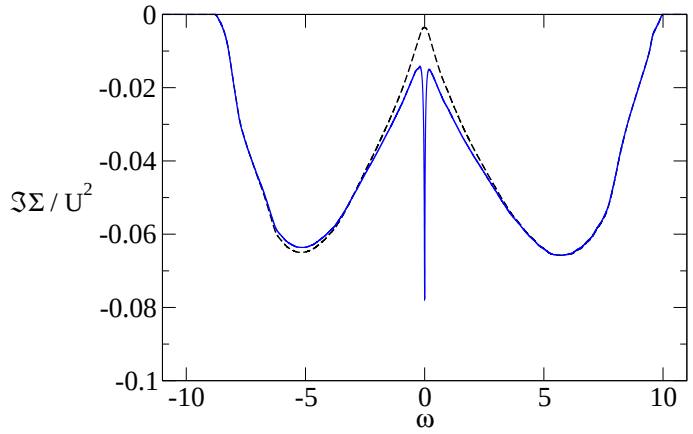

Figure 8: Imaginary part of the self energy $\mathrm{Im}\Sigma(\mathbf{k}_F, \omega)$ normalized by U^2 as a function of ω and $\mathbf{k}_F$ on a hot spot, for parameters $t'/t = -0.1$, $T/t = 0.05$, $U/t = 1.8$ and density $n = 0.92$; the result from the functional RG (solid blue line) is compared to the result from second order perturbation theory (dashed black line) [from Ref. [26]].

peak gradually transforms into a single peak when moving away from the hot spot or van Hove regions, and also upon raising the temperature. In the one-particle irreducible scheme the peak in $\mathrm{Im}\Sigma(\mathbf{k}_F, \omega)$ was found to be partially split by a dip upon moving away from the van Hove point, which leads to a three peak structure in the spectral function [25]. No such splitting was obtained in the Wick ordered functional RG [26]. This discrepancy can be traced back to differences in the approximate flow equations of both schemes, and indicates that higher order corrections become important when the renormalized interactions grow too strong.

One can conclude that self-energy contributions are particularly large near hot spots and tend to destroy Fermi liquid behavior, but the final form of the spectral function requires an analysis beyond the above perturbative truncation of the flow equations.

5 Flow to strong coupling: RG + Mean-Field

Within the one-loop truncation the renormalized two-particle interaction Γ^Λ always diverges at $T = 0$ in one or several momentum channels at a finite energy scale Λ_c, even for a small bare interaction U, resulting in a strong

coupling problem in the low-energy limit. If the two-particle vertex diverges only in the Cooper channel, driven by the particle-particle contribution to the flow, this strong coupling problem can be treated by exploiting Λ_c as a small parameter [28]. The scale Λ_c is exponentially small for a small bare interaction. The formation of a superconducting ground state can then be described essentially by a BCS theory with renormalized input parameters. A method very similar in spirit has been applied very recently to superconductivity in quasi-one-dimensional systems [29].

Here, we use an analogous approach to treat *several* order parameters simultaneously at mean-field level. Near half filling, for $U = 2.5t$ and $t' = -0.2t$ the one-loop flow produces strong interactions in the Cooper channel as well as in the particle-hole channel, the latter being dominated by commensurate (π, π) scattering. We thus concentrate on d-wave superconductivity and antiferromagnetism, which can be treated within a 4×4 Nambu formalism. While the interplay between antiferromagnetic order and d-wave superconductivity has been studied earlier within mean-field theories using models containing pairing interactions [30, 31], we emphasize that we do not introduce such couplings *ad hoc*. Rather, pairing interactions arise within the purely repulsive Hubbard model via the fRG treatment.

In an extended RG framework, spontaneous symmetry breaking can be handled by adding an infinitesimal symmetry breaking term at the beginning of the flow, which is then promoted to a finite order parameter at the scale Λ_c [32]. However, this approach would be extremely involved for the case of competing order parameters we are interested in here. Instead, we stop the one-loop flow at a scale Λ_1 that is small compared to the band width but still safely above the scale Λ_c where the two-particle vertex diverges. At this point the vertex has developed already a pronounced momentum dependence, reflecting in particular magnetic and superconducting correlations. The integration over the remaining modes, below Λ_1, is treated in a mean-field approximation allowing antiferromagnetic and superconducting order. The mean-field theory is defined on a restricted momentum region near the Fermi surface, with $|\epsilon_{\mathbf{k}} - \mu| < \Lambda_1$, and the effective interactions entering the mean-field equations are extracted from Γ^{Λ_1}. Details on this combined RG+MF approach will be presented elsewhere [33]. We now discuss some results for the order parameters.

In Fig. 9 we show the amplitudes of the d-wave superconducting gap (SCG) and the s-wave antiferromagnetic order parameter (AFG) as a function of (electron) density. The latter is computed simultaneously with the order parameters, and thus differs from the initial density of the bare system. For $n = 1$, i.e. at half filling, the AFG is largest, while the SCG is zero. In this case, the system is fully gapped. With decreasing filling the AFG decreases initially roughly linearly, while the SCG remains numerically zero. For electron densities below one, holes appear first in pockets around $(\pi/2, \pi/2)$, which define a surface of low-energy excitations of the non-half

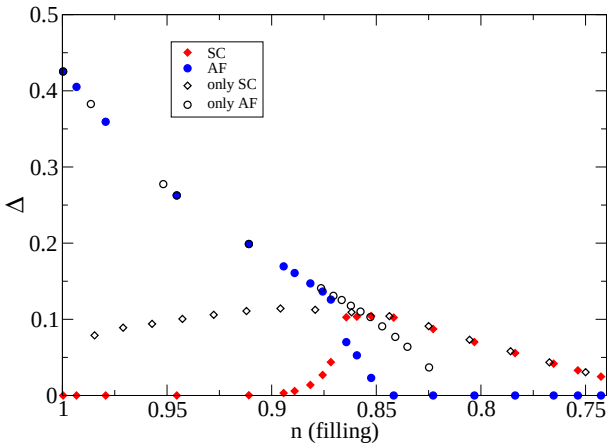

Figure 9: d-wave superconducting order parameter and antiferromagnetic order parameter (in units of t) as a function of density for $U/t = 2.5$ and $t'/t = -0.2$. Filled colored symbols represent the results obtained for the combined theory with two order parameters, while in the calculation leading to the open symbols only one order parameter, either antiferromagnetic or superconducting, was allowed in the mean-field equations.

filled system which increases with larger hole doping. In principle, this residual Fermi surface is always unstable against superconducitivity, due to attraction in the d-wave Cooper channel. However, very close to half-filling, where the pockets are small, the SCG is tiny, since the d-wave attraction is very small near the Brillouin zone diagonal. When the hole pockets are large enough, roughly at $n \approx 0.88$, a sizeable SCG develops, coexisting with a finite AFG. The numerical analysis is rather involved in the coexistence region, and the precise behavior of the order parameters in this regime remains to be clarified. What is clear is that there is a range of densities for which both order parameters are sizable. The coexistence disappears below $n \approx 0.85$. Below this density the AFG truly vanishes, and the SCG is finite and decreases with decreasing filling. The respective results for both order parameters when the other one is set to zero are also shown. When the AFG is set to zero, the SCG persist even at half filling. When the SCG is set to zero, the AFG is enhanced in the coexistence region. In both cases, a finite value for one order parameter leads to a suppression of the other. While these results have been obtained for a weak on-site repulsion, they are in line with the behaviour at stronger coupling as found within variational cluster perturbation theory [34]. There, however, due to finite size effects the possibilty of coexistence on the hole doped side could not be conclusively answered.

Fig. 10 shows the angular dependence of the SCG and the AFG for three selected densities, along with the corresponding hole pockets. Here, ϕ is the

angle with respect to the k_x-axis. Results are shown for a discretisation of 48 patches. For $n = 0.9453$ we obtain a sizeable AFG which has s-wave

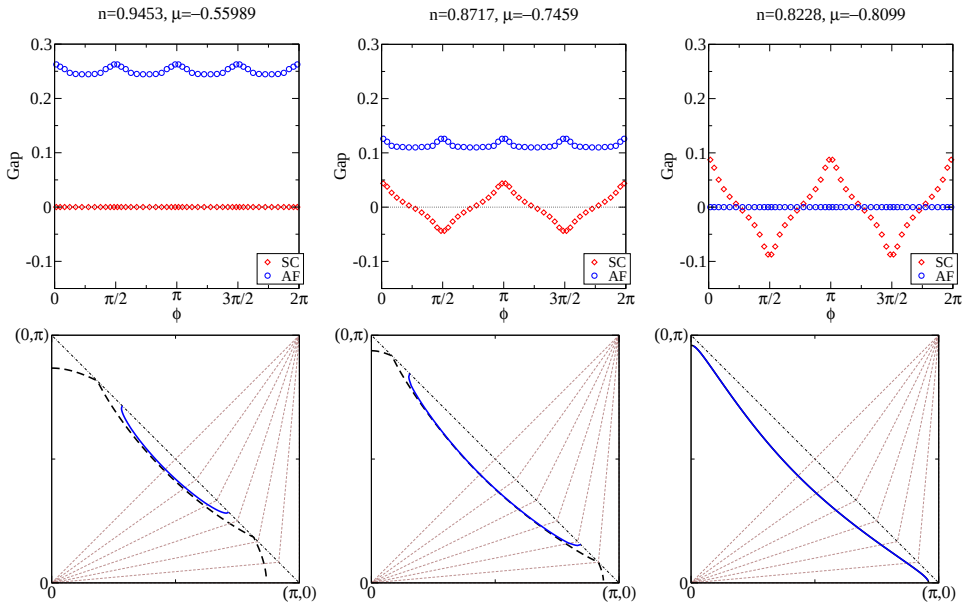

Figure 10: *Top*: d-wave superconducting and antiferromagnetic order parameters at three different values of the chemical potential. *Bottom*: Fermi surfaces in the magnetic Brillouin zone (solid blue lines); in the antiferromagnetic state close to half-filling the Fermi surface forms a hole pocket around $(\pi/2, \pi/2)$. The corresponding bare Fermi surfaces, backfolded with respect to Umklapp surface, are shown as broken lines. The straight lines indicate the patching scheme.

symmetry and is slightly anisotropic. The SCG is practically zero. The oval pocket which opens around $(\pi/2, \pi/2)$ is sizeable, but does not extend far enough to allow for a sizeable d-wave SCG. For $n = 0.8717$ we observe a coexistence of both order parameters. While the AFG is reduced in size compared to the case $n = 0.9453$, its shape remains essentially the same. The pocket extends further away from the zone diagonal, and together with the smaller AFG this allows for a substantial d-wave SCG. In this situation the low-energy excitations are gapped due to the AFG near the points $(\pi, 0)$ and $(0, \pi)$, and gapped due to the SCG along the "Fermi pocket", with nodes along the Brillouin zone diagonals. For an even smaller density of $n = 0.8228$ the AFG vanishes and only a d-wave SCG remains, which extends over the whole Fermi surface, except at the nodal points.

While we have restricted our analysis to superconductivity and antiferromagnetism, there are other instabilities which may arise, such as ferromagnetism (at moderate $|t'/t|$ in the Hubbard model) [35, 36, 37] or a d-wave Pomeranchuk instability of the Fermi surface [38, 39]. The treatment pre-

sented here neglects order parameter fluctuations, which are particularly important in low dimensions. Since we work at $T = 0$ we expect the above results to be qualitatively stable. In a more sophisticated approach order parameter fluctuations can be treated most conveniently by introducing appropriate bosonic fields, as discussed recently for antiferromagnetic order in the half-filled Hubbard model at finite temperature [40].

6 Conclusion

In summary, the functional renormalization group captures many aspects of the complex interplay of magnetic and superconducting correlations in the two-dimensional Hubbard model. In particular, it captures the generation of attractive d-wave Cooper interactions via antiferromagnetic spin correlations already in a one-loop approximation of the vertex flow. Strong correlation effects in the single particle excitations are obtained from the two-loop flow of the self-energy. Magnetic fluctuations suppress spectral weight at hot spots, leading to a pseudogap shape of the spectral function at these points. The strong-coupling problem posed by the divergence of the flow at $T = 0$ is treated approximately by combining the fRG with a mean-field treatment at low energies. Superconducting and antiferromagnetic instabilities are found to compete, with a small range of densities for which both orders can coexist with a sizable order parameter for each.

A more complete analysis of the two-dimensional Hubbard model by renormalization group methods, including also order parameter fluctuations at low energy scales, can be expected to yield further important clues for a better understanding of magnetic and superconducting correlations in high temperature superconductors.

Acknowledgement We thank C. Honerkamp, A.A. Katanin, and M. Salmhofer for valuable discussions, and S. Andergassen for a critical reading of the manuscript.

References

[1] P. W. Anderson, Science **235**, 1196 (1987).

[2] See, for example, D. J. Scalapino, Phys. Rep. **250**, 329 (1995).

[3] K. Miyake, S. Schmitt-Rink, and C. M. Varma, Phys. Rev. B **34**, 6554 (1986).

[4] D. J. Scalapino, E. Loh, and J. E. Hirsch, Phys. Rev. B **34**, 8190 (1986).

[5] N. E. Bickers, D. J. Scalapino, and R. T. Scalettar, Int. J. Mod. Phys. B **1**, 687 (1987).

[6] N. E. Bickers, D. J. Scalapino, and S. R. White, Phys. Rev. Lett. **62**, 961 (1989).

[7] For reviews of numerical work, see E. Dagotto, Rev. Mod. Phys. **66**, 763 (1994); N. Bulut, Adv. Phys. **51**, 1587 (2002).

[8] H. J. Schulz, Europhys. Lett. **4**, 609 (1987).

[9] I. Dzyaloshinskii, Sov. Phys. JETP **66**, 848 (1987).

[10] P. Lederer, G. Montambaux, and D. Poilblanc, J. Phys. (Paris) **48**, 1613 (1987).

[11] K.G. Wilson and J. Kogut, Phys. Rep. C **12**, 75 (1974).

[12] For a pedagogical introduction, see R. Shankar, Rev. Mod. Phys. **66**, 129 (1994).

[13] M. Salmhofer, Commun. Math. Phys. **194**, 249 (1998); *Renormalization* (Springer 1998).

[14] F.J. Wegner and A. Houghton, Phys. Rev. A **8**, 401 (1973).

[15] J. Polchinski, Nucl. Phys. **B231**, 269 (1984).

[16] C. Wetterich, Phys. Lett. B **301**, 90 (1993).

[17] D. Zanchi and H. J. Schulz, Z. Phys. B **103**, 339 (1997); Europhys. Lett. **44**, 235 (1998); Phys. Rev. B **61**, 13609 (2000).

[18] C.J. Halboth and W. Metzner, Phys. Rev. B **61**, 7364 (2000).

[19] C. Honerkamp, M. Salmhofer, N. Furukawa, and T.M. Rice, Phys. Rev. B **63**, 035109 (2001).

[20] A.P. Kampf and A.A. Katanin, Phys. Rev. B **67**, 125104 (2003).

[21] See, for example, H. J. Schulz, *Phys. Rev. Lett.* **64**, 1445 (1990), where also the choice of δ as a function of doping is discussed.

[22] D. Zanchi, Europhys. Lett. **55**, 376 (2001).

[23] C. Honerkamp and M. Salmhofer, Phys. Rev. B **67**, 174504 (2003).

[24] C. Honerkamp, Eur. Phys. J. B **21**, 81 (2001).

[25] A.A. Katanin and A.P. Kampf, Phys. Rev. Lett. **93**, 106406 (2004).

[26] D. Rohe and W. Metzner, Phys. Rev. B **71**, 115116 (2005).

[27] Hot spots are intersections of the Fermi line and the magnetic Brillouin zone boundary.

[28] J. Feldman, J. Magnen, V. Rivasseau, and E. Trubowitz, *Europhys. Lett.* **24**, 437 (1993).

[29] Y. Fuseya, H. Kohno, and K. Miyake, J. Phys. Soc. Jpn. **74**, 722 (2005).

[30] M. Inui, S. Doniach, P.J. Hirschfeld, and A.E. Ruckenstein, Phys. Rev. B **37**, 2320 (1988).

[31] B. Kyung, Phys. Rev. B **62**, 9083 (2000).

[32] M. Salmhofer, C. Honerkamp, W. Metzner, and O. Lauscher, Prog. Theor. Phys. **112**, 943 (2004).

[33] J. Reiss, D. Rohe, and W. Metzner, in preparation.

[34] D. Sénéchal, P.-L. Lavertu, M.-A. Marois, and A.-M.S. Tremblay, Phys. Rev. Lett. **94**, 156404 (2005).

[35] R. Hlubina, S. Sorella, and F. Guinea, *Phys. Rev. Lett.* **78**, 1343 (1997).

[36] C. Honerkamp and M. Salmhofer, Phys. Rev. Lett. **87**, 187004 (2001).

[37] A.A. Katanin and A.P. Kampf, Phys. Rev. B **68**, 195101 (2003).

[38] C. J. Halboth and W. Metzner, Phys. Rev. Lett. **85**, 5162 (2000).

[39] I. Grote, E. Körding, and F. Wegner, J. Low Temp. Phys. **126**, 1385 (2002).

[40] T. Baier, E. Bick, and C. Wetterich, Phys. Rev. B **70**, 125111 (2004).